# Experimental Overview of the Search for Chiral Effects at RHIC

**Gang Wang**

Department of Physics and Astronomy, University of California, Los Angeles, California 90095, USA

E-mail: gwang@physics.ucla.edu

**Abstract.** In high-energy heavy-ion collisions, various novel transport phenomena in local chiral domains result from the interplay of quantum anomalies with magnetic field and vorticity, and could survive the expansion of the fireball and be detected in experiments. Among these phenomena are the chiral magnetic effect, the chiral vortical effect and the chiral magnetic wave, the experimental searches for which have aroused extensive interest. This review will describe the current status of experimental studies at Relativistic Heavy Ion Collider at BNL, and outline the future work in experiment needed to eliminate the existing uncertainties in the interpretation of the data.

## 1. Introduction

The quark-gluon plasma (QGP) created in high-energy heavy-ion collisions could specify its thermodynamic states by the axial chemical potential $\mu_5$. $\mu_5$ characterizes the imbalance of right-handed and left-handed fermions in a domain. A *chiral* domain that bears a nonzero $\mu_5$ may be created locally in heavy-ion collisions on an event-by-event basis [1, 2, 3, 4, 5, 6]. In a noncentral collision, a strong magnetic field ($B \sim 10^{15}$ T) can be produced (mostly by energetic spectator protons) [2, 3], and will induce an electric current along $\overrightarrow{B}$ in chiral domains, $\overrightarrow{J_e} \propto \mu_5 \overrightarrow{B}$, which is called the chiral magnetic effect (CME) [1, 2]. On average, $\overrightarrow{B}$ is perpendicular to the reaction plane ($\Psi_{\rm RP}$) that contains the impact parameter and the beam momenta. Hence the CME will manifest a charge transport across the RP.

Considering the CME and other modes of collective motions, we Fourier decompose the azimuthal distribution of particles of given transverse momentum ($p_T$) and pseudorapidity ($\eta$):

$$\frac{dN_\alpha}{d\phi} \propto 1 + 2v_{1,\alpha}\cos(\Delta\phi) + 2v_{2,\alpha}\cos(2\Delta\phi) + ... + 2a_{1,\alpha}\sin(\Delta\phi) + ..., \quad (1)$$

where $\phi$ is the azimuthal angle of a particle, and $\Delta\phi = \phi - \Psi_{\rm RP}$. The subscript $\alpha$ (+ or −) denotes the charge sign of the particle. Conventionally $v_1$ is called "directed flow" and $v_2$ "elliptic flow" [7]. $a_1$ ($a_{1,-} = -a_{1,+}$) quantifies the electric charge separation due to the CME.

Another complementary transport phenomenon to the CME has been found and named the chiral separation effect (CSE) [8, 9], in which chiral charges are separated along the axis of the magnetic field in the presence of finite density of vector charge: $\overrightarrow{J_5} \propto \mu_{\rm v}\overrightarrow{B}$. In a chirally symmetric phase, the CME and CSE form a collective excitation, the chiral magnetic wave

(CMW) [10, 11]. The CMW manifests a finite electric quadrupole moment of the collision system, where the "poles" ("equator") of the produced fireball acquire additional positive (negative) charge [10]. There are other chiral magnetic/vortical effects such as the chiral vortical effect (CVE) [12], the chiral electric separation effect (CESE) [13, 14] and the chiral vortical wave (CVW) [15]; see Ref [16] for a recent review on these effects.

## 2. Chiral Magnetic Effect

The experimental searches for the CME have been carried out extensively in the past decade at RHIC [17, 18, 19, 20, 21, 22] and the LHC [23]. From event to event, the signs of the $\mu_5$ values are equally likely, and the signs of finite $a_{1,+}$ and $a_{1,-}$ will flip accordingly, leading to $\langle a_{1,+}\rangle = \langle a_{1,-}\rangle = 0$. One therefore has to search for the CME with charge-separation *fluctuations* perpendicular to the reaction plane, e.g., with a three-point correlator [24], $\gamma \equiv \langle \cos(\phi_\alpha + \phi_\beta - 2\Psi_{\rm RP})\rangle$, averaging over all particles in an event and over all events.

The STAR Collaboration first measured the $\gamma$ correlator with the 1$^{\rm st}$ and 2$^{\rm nd}$ harmonic event planes for Au+Au and Cu+Cu collisions at 62.4 and 200 GeV with data from the 2004/2005/2007 RHIC runs [17, 18, 19]. All the results are in qualitative agreement with the CME: the opposite-charge ($\gamma_{\rm OS}$) and the same-charge ($\gamma_{\rm SS}$) correlations display the "right" ordering. The opposite-charge correlations in Cu+Cu are stronger than those in Au+Au, possibly reflecting the suppression of the correlations among oppositely moving particles in a larger system. Similar $\gamma$ results for 200 GeV Au+Au and 2.76 TeV Pb+Pb were observed by the PHENIX Collaboration [22] and the ALICE Collaboration [23], respectively.

STAR has explored two different correlators, the modulated sign correlator [19] and the charge multiplicity asymmetry correlator [21], whose methodology is similar to the $\gamma$ correlator, and yielded very similar results. PHENIX also employed a multiparticle charge-sensitive correlator [25], and their preliminary results also evidence the charge-separation effect. The background from conventional physics was studied with heavy-ion event generators MEVSIM [26], UrQMD [27] and HIJING [28] (with and without an elliptic flow afterburner implemented). None of these generators could achieve reasonable agreement with the data.

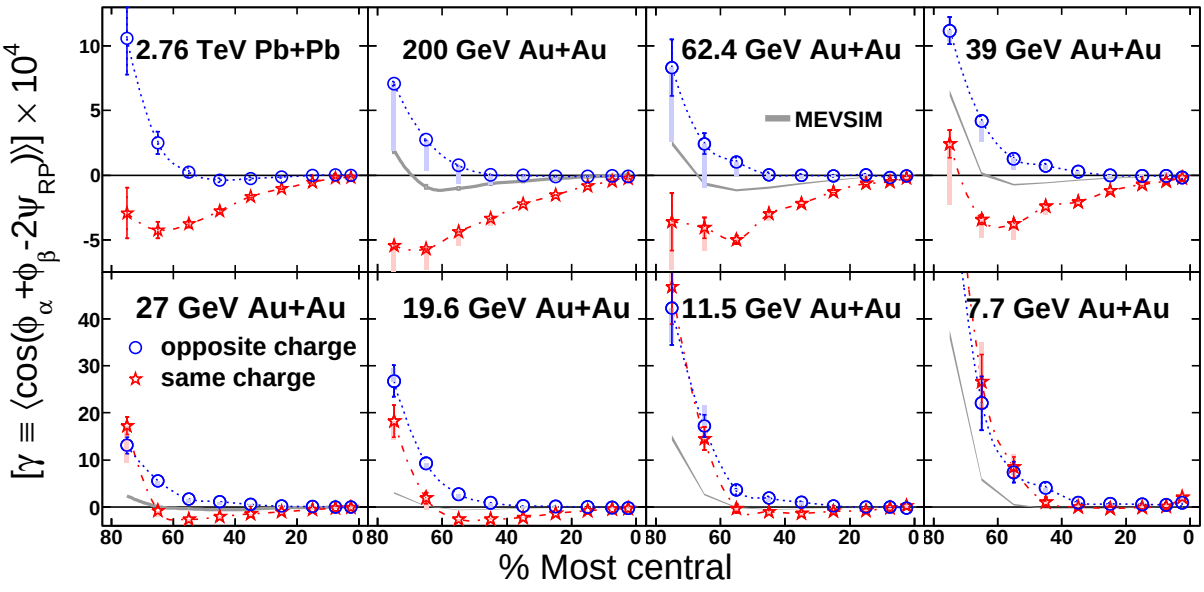


**Figure 1.** $\gamma$ vs centrality for Au+Au collisions at $7.7-200$ GeV [20], and for Pb+Pb collisions at 2.76 TeV [23]. The gray bars reflect the conditions of $\Delta p_T > 0.15$ GeV/$c$ and $\Delta\eta > 0.15$ applied to $\gamma$. Charge independent results from MEVSIM [26] are shown as gray curves.

To further understand the origin of the observed charge separation, Fig. 1 presents $\gamma_{\rm OS}$ and $\gamma_{\rm SS}$ correlators as functions of centrality for Au+Au collisions at $\sqrt{s_{NN}} = 7.7 - 200$ GeV measured by STAR [20], and for Pb+Pb collisions at 2.76 TeV by ALICE [23]. With decreased beam energy, both $\gamma_{\rm OS}$ and $\gamma_{\rm SS}$ tend to rise up starting from peripheral collisions, which seems to be charge independent and can be explained by momentum conservation and elliptic flow [19]. In most cases, the difference between $\gamma_{\rm OS}$ and $\gamma_{\rm SS}$ is still present with the expected ordering, manifesting extra charge-separation fluctuations perpendicular to the reaction plane. The difference between $\gamma_{\rm OS}$ and $\gamma_{\rm SS}$ seems to vanish at low collision energies, but the interpretation involves an ambiguity due to the flow-related background.

One useful tool to study the background is the two-particle correlator, $\delta \equiv \langle \cos(\phi_\alpha - \phi_\beta)\rangle$, which ideally should be protortional to $\langle a_{1,\alpha} a_{1,\beta}\rangle$, but in reality is dominated by backgrounds [20]. The background-subtracted correlator, $H$, can be obtained from the ensemble averages of several observables [20, 29]: $H^\kappa = (\kappa v_2 \delta - \gamma)/(1 + \kappa v_2)$. The major uncertainty in $H$, the coefficient $\kappa$, has been estimated with three approaches to be typically between 1 and 1.5, shown in Fig. 2 [30]. Figure 3 shows $(H_{\rm SS}^{\kappa=1} - H_{\rm OS}^{\kappa=1})$ as a function of beam energy for $30 - 60\%$ Au+Au (Pb+Pb) collisions [20, 23]. $\Delta H^{\kappa=1.5}$ is depicted with the solid line. In both cases of $\kappa$, $\Delta H$ demonstrates a weak energy dependence above 19.6 GeV, and tends to diminish from 19.6 to 7.7 GeV, though the statistical errors are large for 7.7 GeV. This may be explained by the probable domination of hadronic interactions over partonic ones at low energies. A more definitive conclusion may be reached with a more accurate estimation of $\kappa$ and with higher statistics at lower energies in the proposed phase II of the RHIC Beam Energy Scan program, as illustrated by the shaded band in Fig. 3.

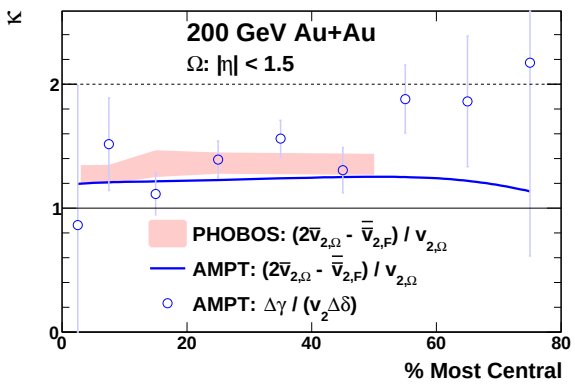


**Figure 2.** (Color online) Estimation of $\kappa$ with three approaches for 200 GeV Au+Au [30].

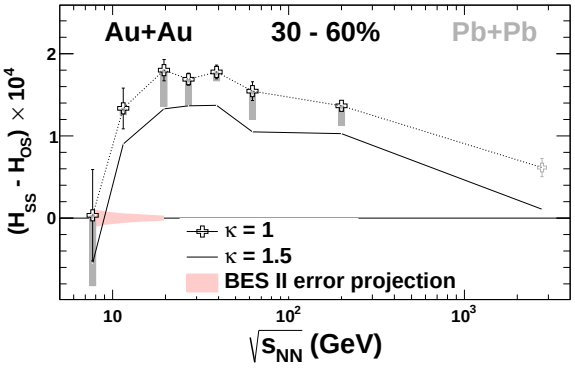


**Figure 3.** (Color online) $\Delta H$ as a function of beam energy for $30 - 60\%$ Au+Au (Pb+Pb) collisions [20, 23]. The systematic errors (gray bars) bear the same meaning as in Fig. 1.

## 3. Chiral Magnetic Wave

The CMW will induce a finite electric quadrupole moment of the collision system, with additional positive (negative) charge at the "poles" ("equator") of the produced fireball [10]. This electric quadrupole, if boosted by radial flow, will lead to charge-dependent elliptic flow. Taking pions as an example, on top of the baseline $v_2^{\rm base}(\pi^\pm)$, the CMW will lead to [10]

$$v_2(\pi^\pm) = v_2^{\rm base}(\pi^\pm) \mp (\frac{q_e}{\bar{\rho}_e}) A_{\rm ch}, \qquad (2)$$

where $q_e$, $\bar{\rho}_e$ and $A_{\rm ch} = (N_+ - N_-)/(N_+ + N_-)$ are the quadrupole moment, the net charge density and the charge asymmetry of the collision event, respectively. Panel (a) of Fig. 4 shows

the example of 30-40% 200 GeV Au+Au, where $\pi^-$ $v_2$ increases with $A_{\rm ch}$ and $\pi^+$ $v_2$ decreases with a similar magnitude of the slope [31]. The $v_2$ difference between $\pi^-$ and $\pi^+$ is fitted with a straight line in panel (b). The slope parameter $r$, or presumably $2q_e/\bar{\rho}_e$ from Eq. 2, is positive and qualitatively consistent with the expectation of the CMW picture.

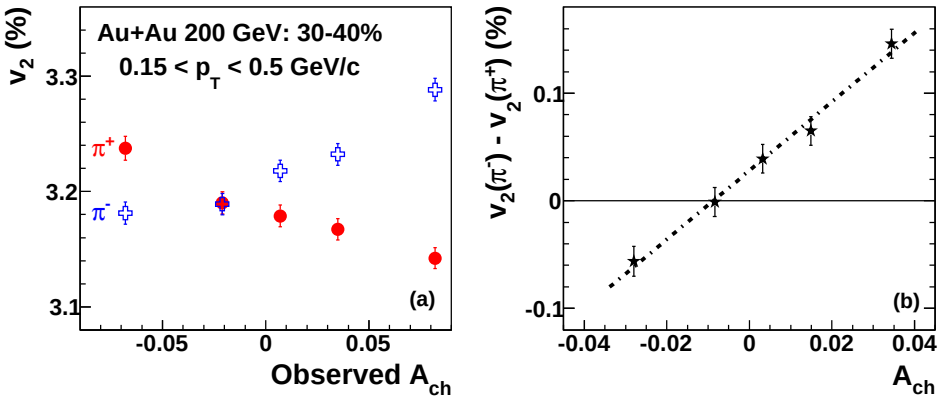


**Figure 4.** (a) pion $v_2$ as a function of observed $A_{\rm ch}$ and (b) $v_2$ difference between $\pi^-$ and $\pi^+$ as a function of corrected $A_{\rm ch}$, for 30-40% Au+Au collisions at 200 GeV [31].

STAR retrieved the slope parameter $r$ as a function of centrality for Au+Au collisions at $7.7-200$ GeV, as shown in Fig. 5 [31]. A similar rise-and-fall trend is observed in the centrality dependence of the slope parameter for all the beam energies except 11.5 and 7.7 GeV, where the slopes are consistent with zero with large statistical uncertainties. A comparison in the slope parameter $r$ between STAR results for 200 GeV Au+Au [31] and ALICE results for 2.76 TeV Pb+Pb [32] shows a striking similarity. For Au+Au collisions at 200 GeV, the slopes extracted from UrQMD events are consistent with zero for the 10-70% centrality range, where the signal from the real data is prominent. Similarly, the AMPT event generator [34, 35] also yields null results. On the other hand, the simplified CMW calculations [33] demonstrate a centrality dependence of the slope parameter similar to the data.

It was pointed out in Ref. [36] that local charge conservation at freeze-out, when convoluted with the characteristic shape of $v_2(\eta)$ and $v_2(p_T)$, may provide a qualitative explanation for the finite $v_2$ slope. A realistic estimate of the contribution of this mechanism turns out to be smaller than the measurment by an order of magnitude [31]. A recent hydrodynamic study [37] suggested that simple viscous transport of charges, combined with certain specific initial conditions, might lead to a sizable contribution to the observed $v_2$ splitting of charged pions. However, certain predictions of this model (e.g. splitting for kaons) appear to be not in line with current experimental information [38].

## 4. Future measurements

The confirmation of the experimental observation of several chiral anomalous effects will bring forth an exciting program to directly study the non-perturbative sector of QCD. Future experimental measurements should aim at more detailed study of the observed signals as well as understanding the background effects. To disentangle the possible CME signal and the flow-related backgrounds, one can utilize experimental setups to either vary the backgrounds with the signal fixed, or vary the signal with the backgrounds fixed. The former approach was carried out by exploiting the prolate shape of the uranium nuclei [39]. However, it was found that the total multiplicity of detected hadrons is far less dependent on the number of binary collisions than expected [40], so it is very hard to isolate tip-tip collisions (that generate small $v_2$) from

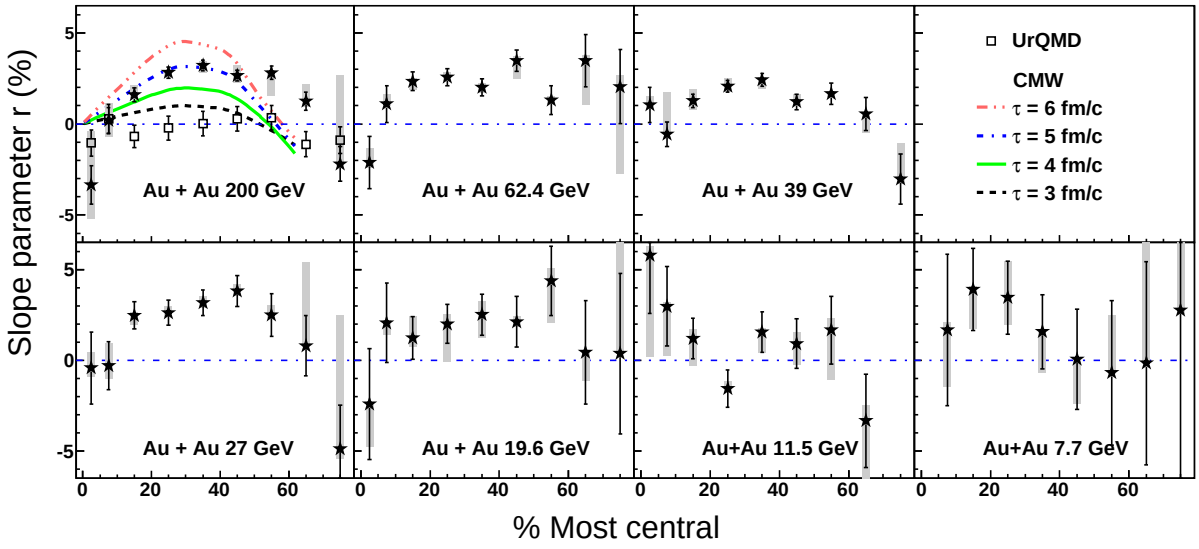


**Figure 5.** The slope parameter $r$ as a function of centrality for Au+Au collisions at $7.7-200$ GeV [31]. The gray bands represent the systematic errors. For comparison, we also show the UrQMD calculations [27] and the calculations of the CMW [33] with different duration times.

body-body collisions (that generate large $v_2$). This significantly reduces the lever arm available to manipulate $v_2$ in order to separate flow backgrounds from the CME.

The latter approach (with the $v_2$-driven backgrounds fixed) can be realized, especially for mid-central/mid-peripheral events, with collisions of isobaric nuclei, such as $^{96}_{44}$Ru and $^{96}_{40}$Zr [39]. Ru+Ru and Zr+Zr collisions at the same beam energy are almost identical in terms of particle production [41], while the charge difference between Ru and Zr nuclei provides a handle on the initial magnetic field. Figure 6(a) shows the projection of $S \equiv N_{\rm part}\Delta\gamma$ for Ru + Ru and Zr + Zr collisions at 200 GeV, as functions of centrality, with the magnetic field and eccentricity obtained for case 1, and the background level $bg = 2/3$ [41]. Here "case 1" (case 2) refers to the information of the nucleus deformity based on e-A scattering experiments [42, 43] (comprehensive model deductions [44]). The statistical errors are estimated based on 400M events for each collision type. The systematic uncertainties in the projection are largely canceled out with the relative difference between Ru + Ru and Zr + Zr, $R_S$, shown in Fig. 6(b); in comparison, the relative difference in eccentricity, $R_{\epsilon_2}$, is also shown. When combining the events of $20-60\%$ centralities, $R_S$ is $5\sigma$ above $R_{\epsilon_2}$ for both parameter cases. Therefore, the isobaric collisions provide a unique test to pin down the underlying physics mechanism for the observed charge separation. As a by-product, $v_2$ measurements in central collisions will discern which information source (case 1 or 2) is more reliable regarding the deformity of the Ru and Zr nuclei.

## References


[1] D. E. Kharzeev, L. D. McLerran and H. J. Warringa, Nucl. Phys. A **803**, 227 (2008).
[2] D. Kharzeev, Phys. Lett. B **633**, 260 (2006).
[3] D. Kharzeev and A. Zhitnitsky, Nucl. Phys. A **797**, 67 (2007).
[4] D. Kharzeev, A. Krasnitz and R. Venugopalan, Phys. Lett. B **545**, 298 (2002).
[5] I. Iatrakis, S. Lin and Y. Yin, Phys. Rev. Lett. **114**, 252301 (2015).
[6] K. Fukushima, D. E. Kharzeev and H. J. Warringa, Phys. Rev. Lett. 104, 212001 (2010).
[7] A. M. Poskanzer and S. Voloshin, Phys. Rev. C **58**, 1671 (1998).
[8] D. T. Son and A. R. Zhitnitsky, Phys. Rev. D **70**, 074018 (2004).
[9] M. A. Metlitski and A. R. Zhitnitsky, Phys. Rev. D **72**, 045011 (2005).
[10] Y. Burnier, D. E. Kharzeev, J. Liao and H.-U. Yee, Phys. Rev. Lett. **107**, 052303 (2011).

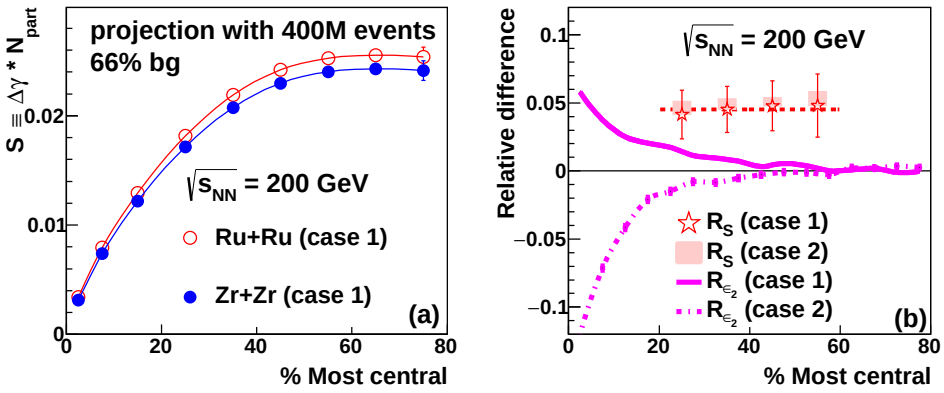


**Figure 6.** Projection of $S \equiv N_{\rm part}\Delta\gamma$ for Ru + Ru and Zr + Zr collisions at $\sqrt{s_{\rm NN}} = 200$ GeV for case 1 (a) and the relative difference (b) versus centrality, assuming the background level to be two thirds [41]. Also shown in panel (b) is the relative difference in the initial eccentricity from the Monte Carlo Glauber [45] simulation (pink solid and dashed lines).


[11] G. M. Newman, JHEP **0601**, 158 (2006).
[12] D. E. Kharzeev and D. T. Son, Phys. Rev. Lett. **106**, 062301 (2011).
[13] X. G. Huang and J. Liao, Phys. Rev. Lett. **110**, 232302 (2013).
[14] Y. Jiang, X. G. Huang and J. Liao, Phys. Rev. D **91**, 045001 (2015).
[15] Y. Jiang, X. G. Huang and J. Liao, Phys. Rev. D **92**, 071501 (2015).
[16] D.E. Kharzeev, J. Liao, S.A. Voloshin and G. Wang, Prog. Part. Nucl. Phys. **88**, 1 (2016).
[17] B. I. Abelev *et al.* [STAR Collaboration], Phys. Rev. Lett. **103**, 251601 (2009).
[18] 7. I. Abelev *et al.* [STAR Collaboration], Phys. Rev. C **81**, 54908 (2010).
[19] L. Adamczyk *et al.* [STAR Collaboration], Phys. Rev. C **88**, 064911 (2013).
[20] L. Adamczyk *et al.* [STAR Collaboration], Phys. Rev. Lett. **113**, 052302 (2014).
[21] L. Adamczyk *et al.* [STAR Collaboration], Phys. Rev. C **89**, 044908 (2014).
[22] N. N. Ajitanand, S. Esumi, R. A. Lacey (PHENIX Collaboration), in: Proc. of the RBRC Workshops, vol.**96**, 230 (2010): "P- and CP-odd ects in hot and dense matter".
[23] B. I. Abelev *et al.* [ALICE Collaboration], Phys. Rev. Lett. **110**, 021301 (2013).
[24] S. A. Voloshin, Phys. Rev. C **70**, 057901 (2004).
[25] N. N. Ajitanand, R. A. Lacey, A. Taranenko and J. M. Alexander, Phys. Rev. C **83**, 011901 (2011).
[26] R. L. Ray and R. S. Longacre, arXiv:nucl-ex/0008009 (2000).
[27] S. A. Bass *et al.*, Prog. Part. Nucl. Phys. **41**, 255 (1998).
[28] M. Gyulassy and X.-N. Wang, Comput. Phys. Commun. **83**, 307 (1994); X.N. Wang and M.Gyulassy, Phys. Rev. D **44**, 3501 (1991).
[29] A. Bzdak, V. Koch and J. Liao, Lect. Notes Phys. **871**, 503 (2013) [arXiv:1207.7327 [nucl-th]].
[30] F. Wen, L. Wen and G. Wang, arXiv:1608.03205 (2016).
[31] L. Adamczyk *et al.* (STAR Collaboration), Phys. Rev. Lett. **114**, 252302 (2015).
[32] J. Adam *et al.* (ALICE Collaboration), Phys. Rev. C **93**, 044903 (2016).
[33] Y. Burnier, D.E. Kharzeev, J. Liao, H.-U. Yee, arXiv:1208.2537 (2012).
[34] B. Zhang, C.M. Ko, B.-A. Li and Z.-W. Lin, Phys. Rev. C **61**, 067901 (2000).
[35] Z.-W. Lin, C.M. Ko, B.-A. Li and B. Zhang, Phys. Rev. C **72**, 064901 (2005).
[36] A. Bzdak and P. Bozek, arXiv:1303.1138 (2013).
[37] Y. Hatta, A. Monnai and B. W. Xiao, Nucl. Phys. A **947**, 155 (2016).
[38] Q.-Y. Shou [STAR Collaboration], Nucl. Phys. A **931**, 758 (2014).
[39] S. A. Voloshin, Phys. Rev. Lett. **105**, 172301 (2010).
[40] L. Adamczyk *et al.* [STAR Collaboration], Phys. Rev. Lett. **115**, 222301 (2015).
[41] W.-T. Deng, X.-G. Huang, G.-L. Ma, G. Wang, arXiv:1607.04697 (2016).
[42] S. Raman, C. W. G. Nestor, Jr and P. Tikkanen, Atom. Data Nucl. Data Tabl. **78**, 1 (2001).
[43] B. Pritychenko, M. Birch, B. Singh and M. Horoi, Atom. Data Nucl. Data Tabl. **107**, 1 (2016).
[44] P. Moller, J. R. Nix, W. D. Myers and W. J. Swiatecki, Atom. Data Nucl. Data Tabl. **59**, 185 (1995).
[45] B. I. Abelev *et al.* [STAR Collaboration], Phys. Rev. C **79**, 034909 (2009).